Modelling Oscillations in the Jet Emission from GRS 1915+105

Ross Collins[1, 2], Christian Kaiser[1], and Simon Cox[2]

[1] Department of Physics and Astrophysics, University of Southampton
[2] Department of Electronics and Computer Science, University of Southampton

Abstract

The variability in the infrared to millimetre emission from microquasar GRS 1915+105 is believed to be totally dominated by the system's relativistic jet. In this paper we develop a time-dependent version of the Blandford & Königl (1979) jet model and apply it to the infrared and millimetre oscillations from GRS 1915+105 observed by Fender & Pooley (2000). The resulting model provides a reasonable description of the observed flux oscillations from GRS 1915+105 and from a fit of the observed time lag between the flux peaks in the infrared and millimetre emission together with the flux normalisation we were able to determine the model parameters for the GRS 1915+105 jet. We find that to achieve the observed flux levels with the model requires an extremely large electron density within the jet to the extent that it is unphysical. We therefore conclude that the Blandford & Königl (1979) model cannot explain these observations, either because it does not provide the correct description of the emission from microquasar jets, or because the observed emission variations do not originate in the jet.

Figure 5 – **Epochs in the Time Evolution of the Jet Emission –** These diagrams compare the electron density profile within the jet to the resulting observed emission, at several different epochs. The left-most plot displays the electron density profile within the jet as a function of the logarithmic radius, which clearly shows the inner-most regions of the jet from where flat spectrum emission originates. The next plot reveals the electron density profile with respect to linear radius within the jet, providing a view which can be more easily compared with observations. The two plots on the right hand side of each diagram show the predicted observable jet emission at 5 wavelengths – infrared (2.2 μm), millimetre (1.3 mm), and three radio wavelengths (15 GHz, 8.3 GHz, and 2.3 GHz). Both the predicted light curve and the broadband (logarithmic) spectrum are displayed. This figure highlights the importance of an emission region which extends over a large range of radii for the creation of a flat spectrum. When the electron injection becomes negligible the effective minimum radius of the emission region rapidly increases, reducing the scale over which the emission region covers, and resulting in the typical 'single radius' self-absorbed synchrotron radiation spectrum.

a) t = **225 s** : A faint flat spectrum extending from beyond infrared down to the millimetre waveband is formed quickly

b) t = **350 s** = t_{max} : The maximum flux level of the flat spectral region is reached as the maximum density electrons are injected, causing the infrared flux to peak

c) t = **435 s** : As the injected electron density decreases the flat region of the spectrum is rapidly destroyed from the high frequency end down to the low frequency end

d) t = **575 s** : With the electron injection now negligible, and the flat spectrum destroyed, a cloud of electron plasma propagates out towards greater radii where the radio emission peaks

e) t = **1750 s** : As this electron plasma cloud reaches greater radii the spectral peak shifts towards lower frequencies

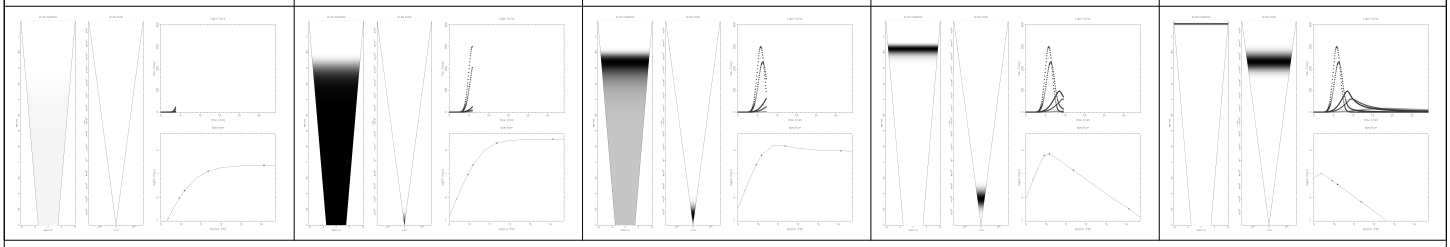

Introduction

The microquasar GRS 1915+105 shows time variability in its emission at all observable wavelengths. Its high energy emission (X-rays) is believed to be created in the inner radii of the system's accretion disc, and its low energy (radio) emission is primarily from synchrotron emitting ejecta located at large radii ($r > 10^{11}$ m) within the system's jet. In this paper we investigate the cause of the variability in the infrared, and millimetre emission from GRS 1915+105 which is believed to originate in the inner regions of the relativistic jet.

The Jet Model

Compact emission from jet sources reveals a flat broadband spectra, believed to be due to synchrotron radiation. The steady-jet model of Blandford & Königl (1979) can recreate flat synchrotron spectra by assuming the following:

- The source population of electrons have a power-law energy distribution as a consequence of acceleration by shocks.
- Emission from electrons is through partially self-absorbed synchrotron radiation.
- Adiabatic expansion of the electron plasma as it propagates towards greater radii gives rise to a conical geometry.
- Electrons do not loose energy from adiabatic decompression or radiative losses. Hence an unexplained, continuous and ubiquitous re-energisation process that can exactly counter the losses is required.

Therefore, the model parameters follow these rules:

- Electron number density, k, will vary with the inverse square of the radius (from restricted, two-dimensional expansion), $k(r) = k_0 (r/r_0)^{-2}$.
- Strength of the magnetic field required for synchrotron emission varies inversely with radius (from flux conservation), $B(r) = B_0 (r/r_0)^{-1}$.
- The jet's half-width as a function of radius is given by, $w(r) = w_0 (r/r_0)$.

The familiar self-absorbed synchrotron radiation spectrum is emitted from every radial point in the jet, which when integrated over an entire emission region, $r_{min} < r < r_{max}$, produces a flat spectrum, as shown in figure 1, over a frequency range $\nu_{min} < \nu < \nu_{max}$, which is dependent upon the emission region length.

The two free parameters in this model are:

- a_0 (= $k_0 B_0^{17/8}$) which controls the frequency range of the flat spectral region.
- B_0 which for a fixed a_0 controls the flux normalisation.

All other model parameters are pre-determined by either observational constraints or theory.

Time Variability

The inclusion of time-dependence to the jet model is achieved by making a_0 a function of time, which represents an individual increase in either of the two physical parameters, B_0 and k_0, or a simultaneous increase in both parameters. We believe that an increase in the injected electron density provides the more appealing physical mechanism of increasing a_0, and therefore $k_0 = k_0(t)$. However, the resulting model is applicable to any physical mechanism that increases a_0. The model now includes:

- An electron density injection profile, $k_0(t)$, which follows a Gaussian profile
- Emission region size determined by $r_{max} = v_j t$, assuming a constant bulk velocity v_j

Example light curves produced by our time-variability model for two different frequencies, ν_1 and ν_2, with the flux normalised to its maximum value are shown in figure 2. The effect of the a_0 parameter upon the resulting flux peaks in the light curve is illustrated in figure 3.

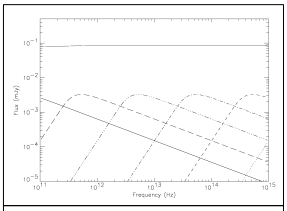

Figure 1 – **Building a flat spectrum** – A flat spectrum is formed from the summation of self-absorbed synchrotron spectra. Here a sample of spectra emitted from electron populations located at increasing radii along the jet reveal the shift of the individual spectra towards lower frequencies. Therefore the frequency extent of the flat spectrum depends upon the size of the emission region. The frequency at which the individual spectra for a given radius peak depends upon the a_0 parameter which is related to the function that describes the optical depth of the jet material as a function of radius.

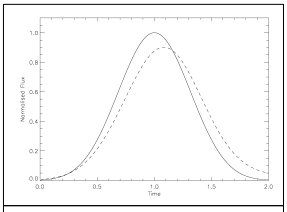

Figure 2 – **The Light Curve Model** – as predicted by our time-variability model for two frequencies ν_2 (solid line), and ν_1 (dashed line), where $\nu_2 > \nu_1$. Time is in units of t_{max}, the time of the peak injected electron density. This model is for a particular value of a_0, and any value of B_0.

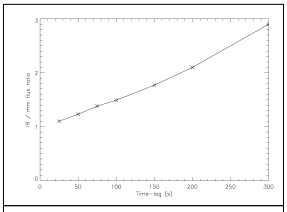

Figure 3 – **The effect of the a_0 parameter** – Increasing the parameter a_0 increases the time lag between flux peaks as well as the flux ratio of the peaks, according to the relationship shown here. This occurs because an increase in a_0 shifts the physical location within the jet emission region where the flat spectral region is created towards greater radii.

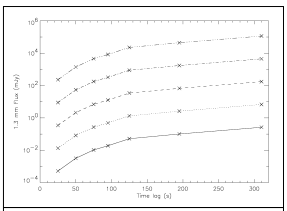

Figure 6 – **Achieving the correct flux normalisation** – Each line in this plot represents the flux normalisation versus time lag relationship for a different value of the peak injected electron density from $k_0 = 10^{36}$, 10^{37}, … to 10^{46} m^{-3}. It is clear that for short time lags it is impossible to recreate the observed flux densities without extremely high values for the electron density.

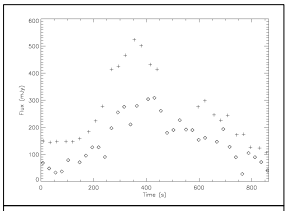

Figure 4 – **The Observation Data** - The first peak in a series of oscillations observed by Fender & Pooley (2000). The crosses denote the de-reddened infrared flux, and the diamonds denote the millimetre flux.

Application to GRS 1915+105

Fender & Pooley (2000) observed oscillations in the emission from GRS 1915+105 at an infrared wavelength (2.2 μm) and a millimetre wavelength (1.3 mm), with flux peaks of similar magnitude for both wavelengths occurring almost simultaneously. We have attempted to model the first peak, which is shown in figure 4. The infrared data has been de-reddened to account for extinction. However, there is an uncertainty in this correction, such that the infrared flux could be up to 40% too luminous.

We assume that the rise time of the infrared flux peak corresponds to the time of peak electron density injection, t_{max} = 350 s. A simulation of our time variability model applied to the GRS 1915+105 jet, with demonstrative values of a_0 and B_0, is shown in figure 5.

In fitting the data, the value of a_0 that predicted a time lag between flux peaks which agreed most closely with the observed time lag of approximately 25 s, was chosen. This was found to be $a_0 = 5.0 \times 10^{27}$ (in SI units), with $r_0 = r_{min} = 10^5$ m, and corresponds to a flux ratio of 1.1 between the peak fluxes of the two frequencies. We attribute the difference between the observed flux ratio and that which is predicted by this model as being due to the observed infrared flux not representing the true infrared flux from the jet. Therefore, we subtract 100 mJy from the infrared data to account for a non-jet background emission component, and then scale the infrared data by a factor of 0.88 to account for a slightly overestimated extinction factor, which gives the exact flux ratio of 1.1. The model's flux normalisation was then fitted to the millimetre data, by adjusting the magnetic field strength parameter, B_0, for which we find $B_0 = 8.0 \times 10^{-7}$ T, with $r_0 = r_{min}$.

For the fitted values of a_0, and B_0, the peak injected electron density at the radius of injection is $k_0 = 5.0 \times 10^{40}$ m^{-3}. This extremely high value is an unavoidable consequence of the model, if such small flux ratios and short time lags are observed over such large frequency ranges. Figure 6 illustrates the need for such large electron densities.

Conclusion

We have discovered that although the Blandford & Königl (1979) model can successfully explain flat broadband spectra, and provide the basis for a reasonable model of time variability, it requires unrealistically high electron densities to agree with the observed flux densities. This result also holds true if the time variability is ignored and the model parameters are determined through the observed flux ratio of the two frequencies at any given time, rather than from the observed time lag between flux peaks of the two frequencies. Therefore either this variable emission does not originate from the jet of GRS 1915+105, or an alternative model is required to explain microquasar jet emission.

References

Blandford, R.D., and Königl, A., 1979, *ApJ*, **232**, 34
Fender, R.P., and Pooley, G.G., 2000, *MNRAS*, **318**, L1

This poster is based upon a paper currently in preparation.
Animations of the time-dependent jet emission model may be found at
http://www.astro.soton.ac.uk/~rsc/ckc02.html